

Investigations of the linear and non-linear flow harmonics using the A Multi-Phase Transport model

Niseem Magdy^{1,*}

¹*Department of Physics, University of Illinois at Chicago, Chicago, Illinois 60607, USA*

The higher-order flow harmonics of the Fourier expansion for the azimuthal distributions of particles are anticipated to be produced by a non-linear response from the lower-order anisotropies, in addition to a linear response from the same-order anisotropies. Detailed study of these higher-order flow harmonics and their non-linear and linear components can be used to constrain the heavy-ion collisions' initial conditions and the system transport properties. The multiparticle azimuthal correlation technique is used within the A Multi-Phase Transport (AMPT) model framework to study the linear and non-linear response to the higher-order flow harmonics, the non-linear response coefficients, and the correlations between different order flow symmetry planes for Au–Au collisions at 200 GeV. The current study shows that the AMPT model can to a good degree describe the experimental measurements and also suggest that conducting detailed measurements over a broad range of system size and beam-energy can serve as an additional constraint for accurate η/s extraction.

Keywords: Collectivity, correlations, shear viscosity

I. INTRODUCTION

Numerous experimental investigations of heavy-ion collisions at the Large Hadron Collider (LHC) and the Relativistic Heavy Ion Collider (RHIC) indicate the creation of the matter predicted by Quantum Chromodynamics (QCD), called Quark-Gluon Plasma (QGP) [1–3], in these collisions. Many of the previous and current experimental investigations in heavy-ion collisions are directed toward a better understanding of the QGP transport properties (especially, η/s) [4–10].

Understanding the QGP transport properties could be achieved via studying the azimuthal anisotropy of particles emitted relative to the collision symmetry planes, (i.e. anisotropic flow). The anisotropic flow measurements are expected to exhibit the viscous hydrodynamic response to the initial spatial distribution formed in the collision's early stages [5, 11–23].

Anisotropic flow can be displayed by the Fourier expansion [24] of the particle azimuthal angle, ϕ , distributions as,

$$\frac{dN}{d\phi} \propto 1 + 2 \sum_{n=1}^{\infty} v_n \cos(n(\phi - \psi_{RP})) \quad (1)$$

where v_n illustrates the value of the n^{th} order flow harmonic, and ψ_{RP} is the reaction plane defined by the beam direction and impact parameter. The v_1 is called directed flow, v_2 is named elliptic flow, and v_3 is termed triangular flow, etc. The earlier investigations of flow correlations and fluctuations [25–35] and higher-order flow coefficients $v_{n>3}$ [19, 27, 32, 36–40], have guided us toward a better understanding of the QGP properties.

In a hydrodynamic-like scenario, anisotropic flow is driven by initial-state energy density spatial anisotropy

characterized by the complex eccentricity vector \mathcal{E}_n [28, 41–44]:

$$\begin{aligned} \mathcal{E}_n &\equiv \varepsilon_n e^{in\Phi_n} \\ &\equiv - \frac{\int dx dy r^n e^{in\varphi} E(r, \varphi)}{\int dx dy r^n E(r, \varphi)}, \quad (n > 1), \end{aligned} \quad (2)$$

where ε_n and Φ_n are the value and azimuthal direction of the n^{th} eccentricity vector, $x = r \cos \varphi$, $y = r \sin \varphi$, φ is the spatial azimuthal angle, and $E(r, \varphi)$ is the initial anisotropic energy density profile [44–46].

The extensively studied v_2 [32, 47–49] and v_3 [37, 50] are, to a good degree, linearly related to ε_2 and ε_3 , respectively [16, 28, 51–57]:

$$v_n = \kappa_n \varepsilon_n, \quad (3)$$

where κ_n is expected to be sensitive to the QGP η/s [37, 58]. Although the lower- and higher-order flow harmonics are expected to result from linear response to the same-order eccentricity, the higher-order flow harmonics, $v_{n>3}$, in addition, have a non-linear response to the lower-order eccentricities $\varepsilon_{n=2,3}$ [21, 45, 46, 59]:

$$\begin{aligned} V_4 &= v_4 e^{i4\psi_4} = \kappa_4 \varepsilon_4 e^{4i\Phi_4} + \kappa_4' \varepsilon_2^2 e^{4i\Phi_2}, \\ &= V_4^{\text{Linear}} + V_4^{\text{NonLinear}}, \\ &= V_4^{\text{Linear}} + \chi_{4,22} V_2 V_2, \end{aligned} \quad (4)$$

where κ_4' carry out knowledge about the medium properties as well as the coupling between the lower and higher order eccentricity harmonics. The terms V_4^{Linear} and $V_4^{\text{NonLinear}}$ are the linear and the non-linear contributions respectively and $\chi_{4,22}$ represents the non-linear response coefficients.

The non-linear contribution to V_4 is expected to display the correlation between different order flow symmetry planes which is expected to shed light on the heavy-ion collisions initial stage dynamics [25, 26, 31, 45, 60–65]. In this work, I studied the η/s impact on the linear and

* niseemm@gmail.com

non-linear contribution of V_4 as well as the coupling constant ($\chi_{4,22}$) and the correlations between different order flow symmetry planes ($\rho_{4,22}$). This current sensitivity study is conducted within the A Multi-phase transport (AMPT) [66] model framework.

The paper is organized as follows. Section II describes the theoretical model (AMPT) and the analysis method employed to compute the linear and non-linear contribution of V_4 . Sec. III, reports the results from this analysis, and is followed by a summary presented in Sec. IV.

II. METHODOLOGY

A. The AMPT model

This investigation is conducted with simulated events for Au–Au collisions at $\sqrt{s_{\text{NN}}} = 200$ GeV, obtained using the AMPT [66] model. Calculations were made for charged hadrons in the transverse momentum span $0.2 < p_T < 2.0$ GeV/ c and the pseudorapidity acceptance $|\eta| < 1.0$. The latter selection mimics the acceptance of the STAR experiment at RHIC.

The AMPT model [66] has been extensively employed to investigate the physics of the relativistic heavy-ion collisions at LHC and RHIC energies [66–73]. In this study, simulations were performed with the string melting option both on and off. In such a scenario when the string melting mechanism is on, hadrons produced using the HIJING model are converted to their valence quarks and anti-quarks, and their evolution in time and space is then formed by the ZPC parton cascade model [74]. The essential components of AMPT constitute of (i) HIJING model [75, 76] initial parton-production stage, (ii) a parton-scattering stage, (iii) hadronization through coalescence followed by (iv) a hadronic interaction stage [77]. In step (ii) the employed parton-scattering cross-sections are estimated according to;

$$\sigma_{pp} = \frac{9\pi\alpha_s^2}{2\mu^2}, \quad (5)$$

where α_s is the QCD coupling constant and μ is the screening mass in the partonic matter. They generally give the expansion dynamics of the A–A collision systems [74]; Within the AMPT framework, the η/s magnitude can be customized via a proper selection of μ and/or α_s for a particular initial temperature T [78].

$$\frac{\eta}{s} = \frac{3\pi}{40\alpha_s^2} \frac{1}{\left(9 + \frac{\mu^2}{T^2}\right) \ln\left(\frac{18 + \mu^2/T^2}{\mu^2/T^2}\right) - 18}, \quad (6)$$

In this work, Au–Au collisions at $\sqrt{s_{\text{NN}}} = 200$ GeV, were simulated with AMPT version ampt-v2.26t9b for a fixed value of $\alpha_s = 0.47$, but the η/s is varied over the range 0.1–0.3 by varying μ in the range $2.26 - 4.2$ fm $^{-1}$ for a temperature $T = 378$ MeV [78]. The AMPT sets which will be shown in this work are given in Tab. I.

| AMPT-set | η/s | String Melting Mechanism |
|----------|----------|--------------------------|
| Set-1 | 0.1 | OFF |
| Set-2 | 0.1 | ON |
| Set-3 | 0.2 | ON |
| Set-4 | 0.3 | ON |

TABLE I. The summary of the AMPT sets used in this work.

The results presented in sec. IIB, were obtained for minimum bias Au–Au collisions at $\sqrt{s_{\text{NN}}} = 200$ GeV. A total of approximately 4.0, 5.0, 4.0, and 3.0 M events of Au–Au collisions were generated with AMPT Set-1, Set-2, Set-3, and Set-4, respectively.

B. Analysis Method

The two- and multiparticle cumulant approaches are employed in the current work. The structure of the cumulant approach is illustrated in Refs. [60, 79], which was extended to the subevents cases in Refs. [80, 81]. In the current work, the two- and multiparticle correlations were constructed using the two-subevents cumulant methods [81], with $\Delta\eta > 0.7$ between the subevents A and B (*i.e.*, $\eta_A > 0.35$ and $\eta_B < -0.35$). The benefit of the two-subevents technique is that it serves to reduce the nonflow correlations [72]. The two- and multiparticle correlations are defined as:

$$v_k^{\text{Inclusive}} = \langle\langle \cos(k(\varphi_1^A - \varphi_2^B)) \rangle\rangle^{1/2}, \quad (7)$$

$$C_{k,nm} = \langle\langle \cos(k\varphi_1^A - n\varphi_2^B - m\varphi_3^B) \rangle\rangle, \quad (8)$$

$$\langle v_n^2 v_m^2 \rangle = \langle\langle \cos(n\varphi_1^A + m\varphi_2^A - n\varphi_3^B - m\varphi_4^B) \rangle\rangle, \quad (9)$$

where $\langle\langle \rangle\rangle$ symbolizes the average over all particles in a single event and then the average over all events, $k = n + m$, and φ_i is the i^{th} particle azimuthal angle.

Using Eqs. (7)-(9), the non-linear contribution to v_4 can be given as [46, 82]:

$$v_4^{\text{NonLinear}} = \frac{C_{4,22}}{\sqrt{\langle v_2^2 v_2^2 \rangle}}, \quad (10)$$

$$\sim \langle v_4 \cos(4\Psi_4 - 2\Psi_2 - 2\Psi_2) \rangle, \quad (11)$$

and the linear contribution to v_4 can be expressed as:

$$v_4^{\text{Linear}} = \sqrt{\langle v_4^{\text{Inclusive}} \rangle^2 - \langle v_4^{\text{NonLinear}} \rangle^2}. \quad (12)$$

Equation (12) implies that the $v_4^{\text{NonLinear}}$ and v_4^{Linear} are independent [46, 72]. The ratio of the $v_4^{\text{NonLinear}}$ to $v_4^{\text{Inclusive}}$ is expected to estimate the correlations between different order flow symmetry planes [83] $\rho_{4,22}$. The $\rho_{4,22}$ can be given as:

$$\rho_{4,22} = \frac{v_4^{\text{NonLinear}}}{v_4^{\text{Inclusive}}} = \langle \cos(4\Psi_4 - 2\Psi_2 - 2\Psi_2) \rangle. \quad (13)$$

The non-linear response coefficients, $\chi_{4,22}$, which quantify the contributions of the coupling to the higher-order anisotropic flow harmonics, are described as:

$$\chi_{4,22} = \frac{v_4^{\text{NonLinear}}}{\sqrt{\langle v_2^2 v_2^2 \rangle}}. \quad (14)$$

III. RESULTS AND DISCUSSION

The extraction of the linear and the non-linear contributions to v_4 relies on the two- and multiparticle correlations. Therefore, it is instructive to investigate the dependence of these variables on the model parameters tabulated in Table I. Fig. 1 shows a comparison of the centrality dependence of $v_n\{2\}$ (a)-(d) for Au–Au collisions at 200 GeV from the AMPT model. The presented $v_n\{2\}$ from the AMPT exhibit a sensitivity to both η/s and whether or not string melting is turned on. They also indicate similar qualitative patterns to the data reported by the STAR collaboration [27, 50] (solid points) over the range of the model parameters given in Table I.

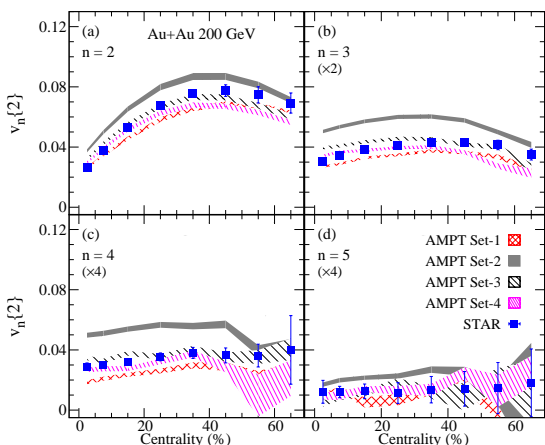


FIG. 1. Centrality dependence of $v_n\{2\}$ computed with the AMPT model for Au–Au collisions at 200 GeV. The solid points represent the experimental data reported by the STAR collaboration [27, 50].

Figure 2 shows a comparison of the centrality dependence of $v_2\{2\}$ (a), $v_2\{4\}$ (b) and the ratios $v_2\{4\}/v_2\{2\}$ (c) for the AMPT model. The results presented in Fig. 2 panels (a) and (b) show that AMPT $v_2\{k\}$ ($k=2$ and 4) are sensitive to model parameters tabulated in Tab. I. They also give similar values and trends to those measured by the STAR experiment [84]. The ratios $v_2\{4\}/v_2\{2\}$, shown in panel (c), work as a figure of merit for the elliptic flow fluctuations strength; $v_2\{4\}/v_2\{2\} \sim 1.0$ correspond to minimal flow fluctuations and decreasing values of $v_2\{4\}/v_2\{2\} < 1.0$ for sizable flow fluctuations. The estimated ratios, which are in good agreement with the experimental ratios, are to within $\sim 2\%$ insensitive to the model choice and the parameter sets given in Tab. I, implying that the flow fluctuations in the AMPT

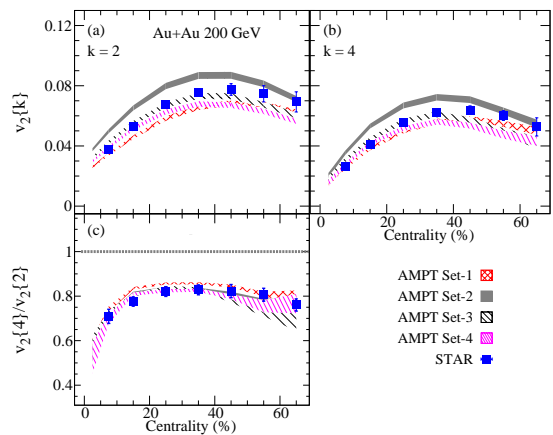


FIG. 2. Centrality dependence of $v_2\{2\}$ (a), $v_2\{4\}$ (b) and $v_2\{4\}/v_2\{2\}$ (c) computed with the AMPT model for Au–Au collisions at 200 GeV. The solid points represent the experimental data reported by the STAR collaboration [27, 37].

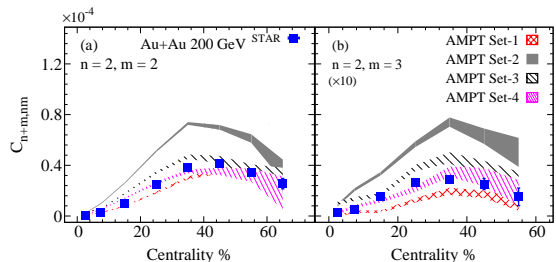


FIG. 3. Comparison of the three-particle correlators, $C_{4,22}$ and $C_{5,23}$ centrality dependence, from the AMPT model for Au–Au collisions at 200 GeV. The solid points represent the experimental data reported by the STAR collaboration [10].

model are eccentricity-driven and are roughly a constant fraction of $v_2\{2\}$.

The three-particle correlators, $C_{4,22}$ and $C_{5,23}$, centrality dependence are shown in Fig. 3 for Au–Au collisions at 200 GeV from the AMPT model. This results indicate that $C_{4,22}$ and $C_{5,23}$ are strongly sensitive to the system η/s and also sensitive to whether or not string melting is turned on. They also show similar patterns to the experimental data reported by the STAR collaboration [10].

The centrality dependence of the inclusive, linear and non-linear v_4 for Au–Au collisions at $\sqrt{s_{NN}} = 200$ GeV from the AMPT model are shown in Fig. 4. The presented measurements indicate that the linear contribution of v_4 which is the dominant contribution to the inclusive v_4 in central collisions has a weak centrality dependence. The presented results show that the inclusive, linear and non-linear v_4 are strongly sensitive to the system η/s . These results are compared to STAR collaboration measurements [10]. The AMPT model simulations indicate similar qualitative patterns to the v_4 measured by the STAR collaboration [10].

The centrality dependence of the non-linear response coefficients, $\chi_{4,22}$, for Au–Au collisions at $\sqrt{s_{NN}} = 200$ GeV, from the AMPT model is presented in Fig. 5(a). The $\chi_{4,22}$ results indicate a weak centrality and η/s de-

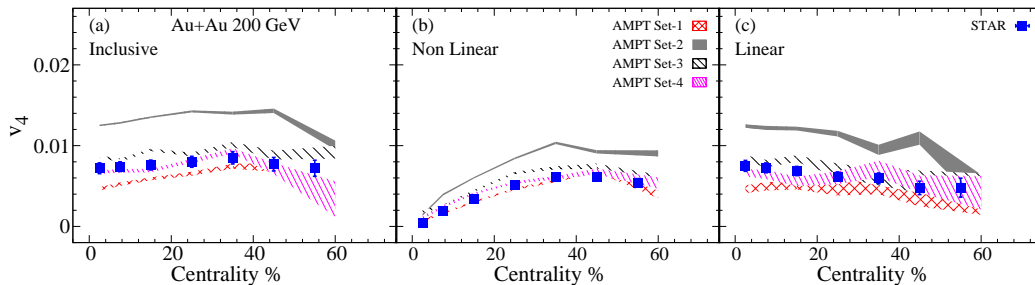


FIG. 4. Centrality dependence of the inclusive, non-linear and linear v_4 obtained with the two-subevents cumulant method from the AMPT model for Au–Au collisions at 200 GeV. The solid points represent the experimental data reported by the STAR collaboration [10].

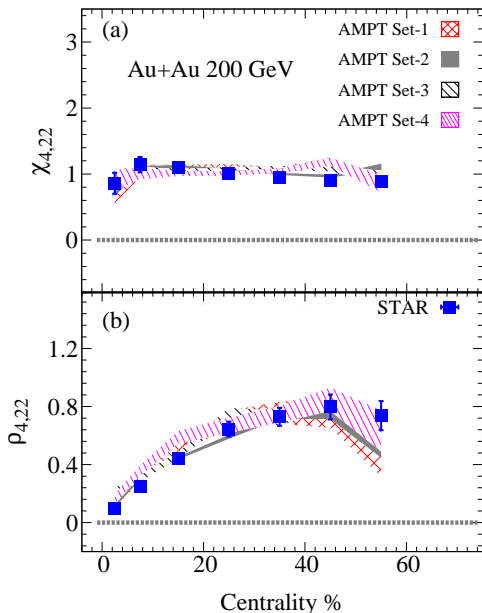


FIG. 5. Comparison of the $\chi_{4,22}$ and $\rho_{4,22}$ obtained from the AMPT model for Au–Au collisions at 200 GeV, as a function of centrality. The solid points represent the experimental data reported by the STAR collaboration [10].

pendence, which implies that (i) the non-linear v_4 centrality dependence is arises from the lower-order flow harmonics and (ii) the $\chi_{4,22}$ is dominated by initial-state eccentricity couplings. The $\chi_{4,22}$ from the AMPT model shows a good agreement with the $\chi_{4,22}$ measured by the STAR experiment [10].

Figure 5(b) shows the centrality dependence of the correlations of the event plane angles, $\rho_{4,22}$, in Au–Au collisions at $\sqrt{s_{NN}} = 200$ GeV from the AMPT model. The $\rho_{4,22}$ results imply stronger event plane correlations in peripheral collisions for all presented AMPT sets. How-

ever, the calculated magnitudes of $\rho_{4,22}$ are shown and found to be independent of η/s . Such observation suggests that the correlation of event plane angles are dominated by initial-state correlations. The $\rho_{4,22}$ from the AMPT model indicate a good agreement with the $\rho_{4,22}$ measured by the STAR collaboration [10].

IV. SUMMARY

In summary, I have presented extensive AMPT model studies to evaluate the viscosity dependence of the linear and non-linear contributions to the v_4 , non-linear response coefficients $\chi_{4,22}$, and the correlations of the event plane angle $\rho_{4,22}$ for Au–Au collisions at $\sqrt{s_{NN}} = 200$ GeV. The presented calculations indicate a large centrality dependence for the non-linear response to v_4 , in contrast, the linear response, that dominates in central collisions, shows a soft centrality dependence. The v_4 AMPT’s calculations show a strong sensitivity to the system viscosity and whether or not string melting is turned on. The dimensionless parameters $\chi_{4,22}$ and $\rho_{4,22}$ show magnitudes and trends which are η/s independent, suggesting that the correlations of event plane angles, as well as the non-linear response coefficients, are dominated by initial-state effects. Based on these AMPT model calculations, I conclude that precise measurements of the linear and non-linear response to the higher-order flow harmonics and their system size and beam-energy dependence can serve as an additional constraint for accurate η/s extraction.

ACKNOWLEDGMENTS

This research is supported by the US Department of Energy, Office of Nuclear Physics (DOE NP), under contracts DE-FG02-94ER40865.

[1] E. V. Shuryak, Phys. Lett. B **78**, 150 (1978).

[2] E. V. Shuryak, Phys. Rept. **61**, 71 (1980).

- [3] B. Muller, J. Schukraft, and B. Wyslouch, *Ann. Rev. Nucl. Part. Sci.* **62**, 361 (2012).
- [4] E. Shuryak, *Prog. Part. Nucl. Phys.* **53**, 273 (2004).
- [5] P. Romatschke and U. Romatschke, *Phys.Rev.Lett.* **99**, 172301 (2007).
- [6] M. Luzum and P. Romatschke, *Phys.Rev.* **C78**, 034915 (2008).
- [7] P. Bozek, *Phys. Rev. C* **81**, 034909 (2010).
- [8] S. Acharya *et al.* (ALICE), *Phys. Rev. Lett.* **123**, 142301 (2019).
- [9] S. Acharya *et al.* (ALICE), *JHEP* **05**, 085 (2020).
- [10] J. Adam *et al.* (STAR), *Phys. Lett. B* **809**, 135728 (2020).
- [11] U. W. Heinz and P. F. Kolb, *Statistical QCD. Proceedings, International Symposium, Bielefeld, Germany, August 26-30, 2001*, *Nucl. Phys. A* **702**, 269 (2002).
- [12] T. Hirano, U. W. Heinz, D. Kharzeev, R. Lacey, and Y. Nara, *Phys.Lett.* **B636**, 299 (2006).
- [13] P. Huovinen, P. F. Kolb, U. W. Heinz, P. V. Ruuskanen, and S. A. Voloshin, *Phys. Lett.* **B503**, 58 (2001).
- [14] T. Hirano and K. Tsuda, *Phys. Rev.* **C66**, 054905 (2002).
- [15] M. Luzum, *J. Phys.* **G38**, 124026 (2011).
- [16] H. Song, S. A. Bass, U. Heinz, T. Hirano, and C. Shen, *Phys. Rev. Lett.* **106**, 192301 (2011), [Erratum: *Phys. Rev. Lett.*109,139904(2012)].
- [17] J. Qian, U. W. Heinz, and J. Liu, *Phys. Rev.* **C93**, 064901 (2016).
- [18] N. Magdy (STAR), *Proceedings, 11th International Workshop on Critical Point and Onset of Deconfinement (CPOD2017): Stony Brook, NY, USA, August 7-11, 2017*, *PoS CPOD2017*, 005 (2018).
- [19] N. Magdy (STAR), *Proceedings, 16th International Conference on Strangeness in Quark Matter (SQM 2016): Berkeley, California, United States, J. Phys. Conf. Ser.* **779**, 012060 (2017).
- [20] B. Schenke, S. Jeon, and C. Gale, *Phys.Lett.* **B702**, 59 (2011).
- [21] D. Teaney and L. Yan, *Phys. Rev.* **C86**, 044908 (2012).
- [22] F. G. Gardim, F. Grassi, M. Luzum, and J.-Y. Ollitrault, *Phys.Rev.Lett.* **109**, 202302 (2012).
- [23] R. A. Lacey, D. Reynolds, A. Taranenko, N. N. Ajitanand, J. M. Alexander, F.-H. Liu, Y. Gu, and A. Mwai, *J. Phys.* **G43**, 10LT01 (2016).
- [24] A. M. Poskanzer and S. A. Voloshin, *Phys. Rev.* **C58**, 1671 (1998).
- [25] J. Adam *et al.* (STAR), *Phys. Lett.* **B783**, 459 (2018).
- [26] J. Adam *et al.* (ALICE), *Phys. Rev. Lett.* **117**, 182301 (2016).
- [27] L. Adamczyk *et al.* (STAR), *Phys. Rev.* **C98**, 034918 (2018).
- [28] Z. Qiu and U. W. Heinz, *Phys. Rev.* **C84**, 024911 (2011).
- [29] A. Adare *et al.* (PHENIX), *Phys. Rev. Lett.* **107**, 252301 (2011).
- [30] G. Aad *et al.* (ATLAS), *Phys. Rev.* **C90**, 024905 (2014).
- [31] G. Aad *et al.* (ATLAS), *Phys. Rev.* **C92**, 034903 (2015).
- [32] N. Magdy (STAR), *Proceedings, 27th International Conference on Ultrarelativistic Nucleus-Nucleus Collisions (Quark Matter 2018): Venice, Italy, May 14-19, 2018*, *Nucl. Phys. A* **982**, 255 (2019).
- [33] B. Alver *et al.* (PHOBOS), *Phys. Rev.* **C77**, 014906 (2008).
- [34] B. Alver *et al.* (PHOBOS), *Phys. Rev.* **C81**, 034915 (2010).
- [35] J.-Y. Ollitrault, A. M. Poskanzer, and S. A. Voloshin, *Phys. Rev.* **C80**, 014904 (2009).
- [36] N. Magdy (STAR), (2019), arXiv:1909.09640 [nucl-ex].
- [37] J. Adam *et al.* (STAR), *Phys. Rev. Lett.* **122**, 172301 (2019).
- [38] L. Adamczyk *et al.* (STAR), *Phys. Rev.* **C98**, 014915 (2018).
- [39] B. Alver and G. Roland, *Phys. Rev.* **C81**, 054905 (2010), [Erratum: *Phys. Rev.C*82,039903(2010)].
- [40] S. Chatrchyan *et al.* (CMS), *Phys. Rev.* **C89**, 044906 (2014).
- [41] B. H. Alver, C. Gombeaud, M. Luzum, and J.-Y. Ollitrault, *Phys. Rev.* **C82**, 034913 (2010).
- [42] H. Petersen, G.-Y. Qin, S. A. Bass, and B. Muller, *Phys. Rev.* **C82**, 041901 (2010).
- [43] R. A. Lacey, R. Wei, N. N. Ajitanand, and A. Taranenko, *Phys. Rev.* **C83**, 044902 (2011).
- [44] D. Teaney and L. Yan, *Phys. Rev.* **C83**, 064904 (2011).
- [45] R. S. Bhalerao, J.-Y. Ollitrault, and S. Pal, *Phys. Lett.* **B742**, 94 (2015).
- [46] L. Yan and J.-Y. Ollitrault, *Phys. Lett.* **B744**, 82 (2015).
- [47] L. Adamczyk *et al.* (STAR), *Phys. Rev. C* **94**, 034908 (2016).
- [48] L. Adamczyk *et al.* (STAR), *Phys. Rev. C* **93**, 014907 (2016).
- [49] L. Adamczyk *et al.* (STAR), *Phys. Rev. Lett.* **115**, 222301 (2015).
- [50] L. Adamczyk *et al.* (STAR), *Phys. Rev. Lett.* **116**, 112302 (2016).
- [51] H. Niemi, G. S. Denicol, H. Holopainen, and P. Huovinen, *Phys. Rev.* **C87**, 054901 (2013).
- [52] F. G. Gardim, J. Noronha-Hostler, M. Luzum, and F. Grassi, *Phys. Rev.* **C91**, 034902 (2015).
- [53] J. Fu, *Phys. Rev.* **C92**, 024904 (2015).
- [54] H. Holopainen, H. Niemi, and K. J. Eskola, *Phys. Rev.* **C83**, 034901 (2011).
- [55] G.-Y. Qin, H. Petersen, S. A. Bass, and B. Muller, *Phys.Rev.* **C82**, 064903 (2010).
- [56] C. Gale, S. Jeon, B. Schenke, P. Tribedy, and R. Venugopalan, *Phys. Rev. Lett.* **110**, 012302 (2013).
- [57] P. Liu and R. A. Lacey, *Phys. Rev. C* **98**, 021902 (2018).
- [58] U. Heinz and R. Snellings, *Ann. Rev. Nucl. Part. Sci.* **63**, 123 (2013).
- [59] F. G. Gardim, F. Grassi, M. Luzum, and J.-Y. Ollitrault, *Phys. Rev. C* **85**, 024908 (2012).
- [60] A. Bilandzic, C. H. Christensen, K. Gulbrandsen, A. Hansen, and Y. Zhou, *Phys. Rev.* **C89**, 064904 (2014).
- [61] Y. Zhou, *Adv. High Energy Phys.* **2016**, 9365637 (2016).
- [62] Z. Qiu and U. Heinz, *Phys. Lett.* **B717**, 261 (2012).
- [63] D. Teaney and L. Yan, *Phys. Rev.* **C90**, 024902 (2014).
- [64] H. Niemi, K. J. Eskola, and R. Paatelainen, *Phys. Rev.* **C93**, 024907 (2016).
- [65] Y. Zhou, K. Xiao, Z. Feng, F. Liu, and R. Snellings, *Phys. Rev.* **C93**, 034909 (2016).
- [66] Z.-W. Lin, C. M. Ko, B.-A. Li, B. Zhang, and S. Pal, *Phys. Rev.* **C72**, 064901 (2005).
- [67] G.-L. Ma and Z.-W. Lin, *Phys. Rev.* **C93**, 054911 (2016).
- [68] M. R. Haque, M. Nasim, and B. Mohanty, *J. Phys. G* **46**, 085104 (2019).
- [69] P. P. Bhaduri and S. Chattopadhyay, *Phys. Rev. C* **81**, 034906 (2010).

- [70] M. Nasim, L. Kumar, P. K. Netrakanti, and B. Mohanty, Phys. Rev. C **82**, 054908 (2010).
- [71] J. Xu and C. M. Ko, Phys. Rev. C **83**, 021903 (2011).
- [72] N. Magdy, O. Evdokimov, and R. A. Lacey, J. Phys. G **48**, 025101 (2020).
- [73] Y. Guo, S. Shi, S. Feng, and J. Liao, Phys. Lett. B **798**, 134929 (2019).
- [74] B. Zhang, Comput. Phys. Commun. **109**, 193 (1998).
- [75] X.-N. Wang and M. Gyulassy, Phys. Rev. **D44**, 3501 (1991).
- [76] M. Gyulassy and X.-N. Wang, Comput. Phys. Commun. **83**, 307 (1994).
- [77] B.-A. Li and C. M. Ko, Phys. Rev. **C52**, 2037 (1995).
- [78] J. Xu and C. M. Ko, Phys. Rev. C **83**, 034904 (2011).
- [79] A. Bilandzic, R. Snellings, and S. Voloshin, Phys. Rev. **C83**, 044913 (2011).
- [80] K. Gajdošová (ALICE), *Proceedings, 26th International Conference on Ultra-relativistic Nucleus-Nucleus Collisions (Quark Matter 2017): Chicago, Illinois, USA, February 5-11, 2017*, Nucl. Phys. **A967**, 437 (2017).
- [81] J. Jia, M. Zhou, and A. Trzupek, Phys. Rev. **C96**, 034906 (2017).
- [82] R. S. Bhalerao, J.-Y. Ollitrault, and S. Pal, Phys. Rev. **C88**, 024909 (2013).
- [83] S. Acharya *et al.* (ALICE), Phys. Lett. **B773**, 68 (2017).
- [84] J. Adams *et al.* (STAR), Phys. Rev. C **72**, 014904 (2005).